see commentary on page 1295

Effects of glomerular filtration rate on Ficoll sieving coefficients (θ) in rats

C Rippe[1], D Asgeirsson[1], D Venturoli[1], A Rippe[1] and B Rippe[1]

[1]*Department of Nephrology, Clinical Sciences, University Hospital of Lund, Lund Univeristy, Lund, Sweden*

The purpose of the present study was to assess the role of diffusion and convection during filtration of Ficoll across the glomerular filter by comparing glomerular sieving coefficients (θ) to neutral fluorescein isothiocyanate (FITC)-Ficoll 70/400 obtained at low (hydropenic) vs raised (normal) glomerular filtration rates (GFRs). The θ for FITC-Ficoll was determined in anesthetized Wistar rats (304 ± 18 g) following laparotomy and cannulation of the ureters, used for urine sampling. After surgery, GFR was 1.2 ± 0.16 ml/min (± s.e.), assessed using the plasma to urine clearance of FITC-inulin and ^{51}Cr-ethylenediaminetetraacetic acid. FITC-Ficoll 70/400 was infused intravenously (i.v.) following an initial bolus dose. To raise GFR, to an average of ~2 ml/min, 5 ml of serum together with glucagon (3 μg/min) was given i.v. FITC-inulin and FITC-Ficoll were determined in plasma and urine using size-exclusion high-performance liquid chromatography. The θ for Ficoll as a function of Stokes–Einstein radius was significantly reduced in the range of 13–43 Å when GFR was raised. The maximal θ lowering effect, in relative terms, of raising GFR was obtained for a Ficoll a_e of ~32 Å. For Ficoll$_{36\,Å}$ (cf. albumin), θ was reduced from 0.111 ± 0.009 to 0.081 ± 0.012 ($P < 0.05$; $n = 7$) for the GFR increment imposed. The reduction in θ for Ficoll after raising GFR indicates the presence of a high diffusive component of glomerular Ficoll filtration in rats *in vivo* and contradicts the notion of a significant concentration polarization effect in the glomerular filter upon Ficoll molecules < 50 Å in radius.

Kidney International (2006) **69,** 1326–1332. doi:10.1038/sj.ki.5000027; published online 4 January 2006

KEYWORDS: capillary permeability; macromolecules; reflection coefficient; filtration barrier; concentration polarization; albumin

Correspondence: *C Rippe, Department of Nephrology, Clinical Sciences, University Hospital of Lund, Lund University, Lund SE-221 85, Sweden. E-mail: Catarina@rippe.se*

Received 28 April 2005; revised 1 July 2005; accepted 12 August 2005; published online 4 January 2006

The glomerular barrier freely filters small solutes to the primary urine, while almost completely retaining large and negatively charged proteins in plasma.[1] This specialized filter is composed of three layers: the fenestrated capillary wall with its glycocalyx, the glomerular basement membrane, and the podocyte slit diaphragm (PSD). The glomerular basement membrane is conceivably a rigid membrane, constructed of a network of type IV collagen molecules. The podocytes extend around the capillaries with interdigitating foot processes connected to each other via the PSD, containing a number of different molecules, of which nephrin was the first to be discovered.[2] The general idea of which portion is the most important as a filtration barrier varies greatly among different research groups.[1] Some authors believe that the main filter is represented by the PSD,[2–4] while recent glomerular protein sieving data in intact rats indicate that size separation may occur already in the 'early' portion of the glomerular basement membrane close to the plasma side.[5] The charge selectivity of the membrane is conceived to be located mainly in the highly negatively charged endothelial glycocalyx.[3,6]

If most of the sieving barrier were located in the PSD, this would lead to protein upconcentration in the 'late' portion of the filter, just beneath the PSD, denoted 'concentration polarization', during high glomerular filtration rates (GFRs) (like a 'traffic jam').[7] This increased concentration of proteins in the glomerular basement membrane would, in turn, produce an increased sieving coefficient (θ) for large proteins at high GFRs. However, if concentration polarization is negligible, the effect of an increased GFR would be a reduction in the relative amount of diffusion, as compared to convection, of macromolecules in the membrane, and this would instead lead to a reduction in θ with increases in GFR, at least for smaller macromolecules (radius 20–40 Å).[8–12] In a recent study, Lund *et al.*[5] indeed found a reduction in θ for proteins with increases in GFR, suggesting the absence of concentration polarization in the glomerular basement membrane. This study seemed to confirm the earlier 'classic' study of Chang *et al.*,[8] who also noted a reduced θ for dextran fractions ranging between 18 and 44 Å in radius when GFR was increased. However, the use of dextrans in glomerular sieving studies can be criticized. Dextrans are highly flexible and elongated polysaccharides, which seem to be able to penetrate pores that are even smaller than their

Stokes—Einstein (SE) radius,[13] indicating that these molecules are hyperpermeable.[14,15] Ficoll is a highly branched and crosslinked polysaccharide, exhibiting an almost spherical (ellipsoidal) conformation, similar to that of a globular protein. Like dextran, it is inert, uncharged, highly polydisperse, and not processed by the proximal tubules. Owing to these characteristics, Ficoll is today regarded as the 'golden standard' for assessing the barrier characteristics of the glomerular filter.[1]

The major aim of the present study was to investigate the behavior of θ for Ficoll as a function of GFR, in order to assess the relationships between diffusive and convective processes across the glomerular membrane and to test the hypothesis whether concentration polarization in the glomerular sieving barrier may occur at raised (normal) levels of GFRs. Does Ficoll behave in a way similar to proteins and dextrans, hence, demonstrating a fall in θ with an elevated GFR, consistent with a high diffusive component and the presence of a marked size-separation effect occurring 'early' in the filter, that is, close to the plasma compartment?

RESULTS

The relationships between $\log\theta$ for Ficoll and molecular radius curves (13–75 Å, 340 data points), at the low (hydropenic) and elevated (normal) GFRs, are given in Figure 1. Raising GFR from 1.16 ± 0.17 to 2.03 ± 0.17 ml/min ($n=7$) significantly reduced θ for Ficoll molecules of radius 13–43 Å. This reduction in θ is particularly evident from Figure 2a, where the θ vs molecular radius (13–45 Å) are plotted in a linear diagram. The ratio of θ values obtained at 2 ml/min of GFR to those obtained at 1.2 ml/min with the 95% confidence interval indicates that the maximal difference in θ was obtained at 32 Å (Figure 2b).

The best-curve fit of θ vs a_e using the two-pore theory and log-normal distribution at the two levels of GFR is shown in Figure 3a and b, respectively. We were able to obtain a perfect fit of data to theory for the two different GFR levels with the log-normal distributed pore model (Figure 3b). However, the Ficoll θ values in the a_e range between 50 and 60 Å were poorly fitted by the two-pore theory (Figure 3a). This is also evident from the mean square-root percentage error for the two models, being 230 and 250% at 'hydropenic' vs 'normal' GFR, respectively, for the two-pore model, while being only 22.2 and 45.2%, respectively, for the log-normal distribution. The parameters obtained for each model are listed in Tables 1a and b. As evident from Table 1, raising GFR from hydropenic to normal values did not affect any of the measured membrane parameters significantly. Furthermore, applying the two-pore model, the small pore radius became much higher and $A_0/\Delta X$ much lower than previously determined for neutral proteins.[5] However, the average pore radius and $A_0/\Delta X$ obtained with the log-normal distributed model were no different from the corresponding values obtained using the two-pore model applied to neutral protein data in a previous study.[5]

Raising GFR from 1.2 to 2.0 ml/min ($n=7$), according to the two-pore model, implies a 15–20% reduction in θ for Ficoll fractions of radius 13–45 Å. Our measured sieving data for Ficoll reflected an even larger drop in θ than expected when simulated for the two-pore model (setting $A_0/\Delta X$ at

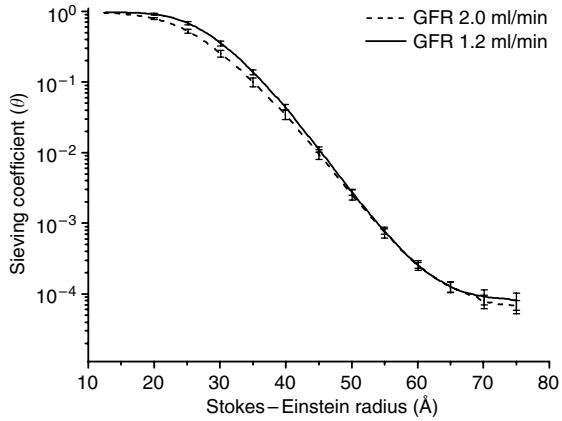

Figure 1 | Sieving coefficients (θ) to Ficoll ($n=7$) for a wide range SE radii (a_e) at a 'normal' GFR (GFR $=2.03\pm0.17$ ml/min; $n=7$) and at 'hydropenic' GFR (GFR $=1.16\pm0.17$; $n=7$), plotted in a semilog diagram.

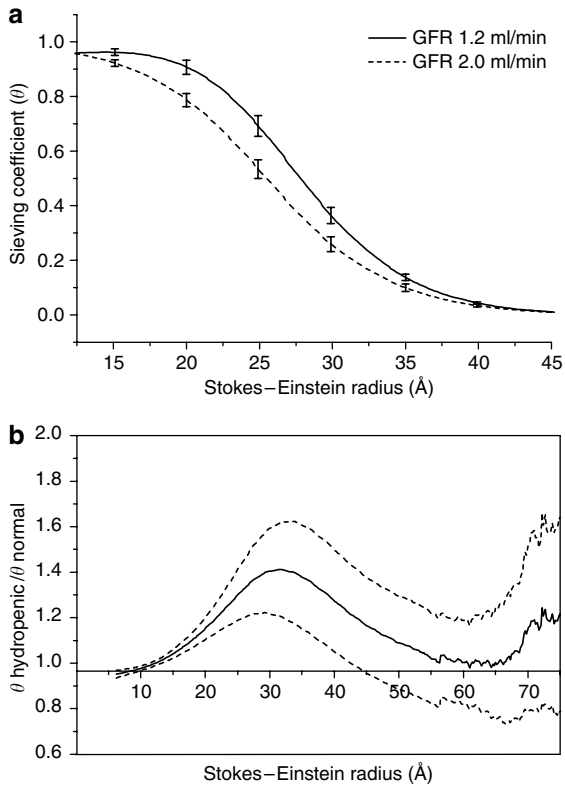

Figure 2 | (a) A linear plot showing the effects of a GFR increment on θ to Ficoll for a_e 13–45 Å ($n=7$). (**b**) θ ratio between values obtained for 1.6 ml/min ('hydropenic' rats) vs 2.03 ml/min of GFR ('normal' rats), respectively. The sieving coefficients were significantly lower at an elevated GFR between 13 and 43 Å as shown by the 95% confidence interval (----), as the θ ratio was significantly different from unity in this interval.

390 000 cm). For $Ficoll_{25\,Å}$, the theoretically predicted reduction in θ from the two-pore theory, when GFR is raised from 1.2 to 2.0 ml/min, is from 0.65 to 0.55 using the parameters listed in Table 1a. However, measured values were 0.68 ± 0.038 and 0.52 ± 0.034, respectively. For $Ficoll_{36\,Å}$ (cf. albumin), predicted θ values are 0.11 vs 0.10, whereas the measured data were 0.111 ± 0.009 vs 0.081 ± 0.012. The negative trend of the relationship between θ vs GFR is illustrated in Figure 4 for four different molecular radii, namely 20, 25, 30, and 36 Å.

Raising GFR from 1.2 to 1.9 ml/min ($n = 7 + 3$; see Materials and Methods) did not significantly affect θ for molecules in the range of 50–70 Å. However, for molecules larger than 70 Å (in a_e), there was a tendency toward a reduced θ, even though this tendency did not reach statistical significance. This is illustrated in Figure 2b, showing that the 95% confidence interval of the θ ratio for low vs high GFRs was not significantly different from unity for $a_e > 43$ Å. Furthermore, the 95% confidence interval widened considerably for a_e values >70 Å, reflecting the high variability in θ measurements for the largest molecules.

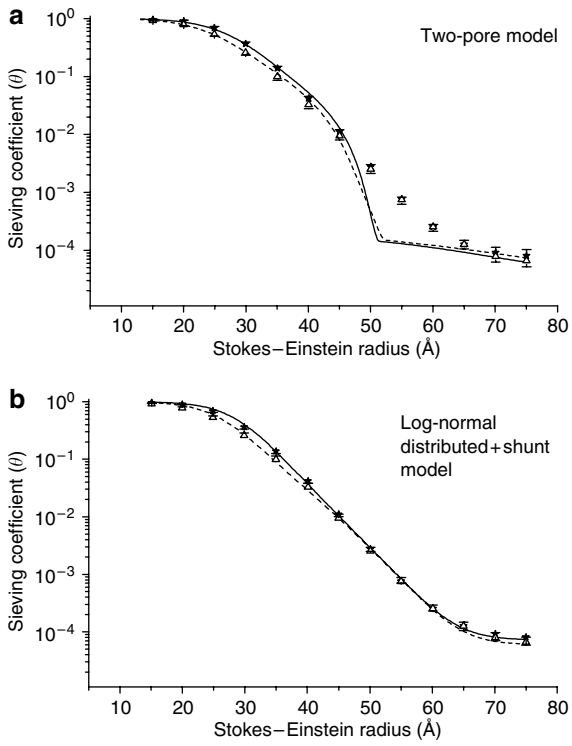

Figure 3 | (a) Ficoll sieving coefficients vs SE radius, with a 5 Å interval, at GFR 1.2 ml/min (★, +SE) and at GFR 2.0 ml/min (△, -SE), together with the simulated best-curve fits using the two-pore model (— and ----, respectively, at the GFR levels investigated). (**b**) Experimental data for sieving coefficients at GFR 1.2 ml/min (★, +SE) and at GFR 2.0 ml/min (△, −SE), together with the simulated best-curve fits using the log-normal distributed model + shunt (— and ----, respectively). A near-perfect fit of the log-normal distributed pore model to measured Ficoll data was obtained at the two GFR levels.

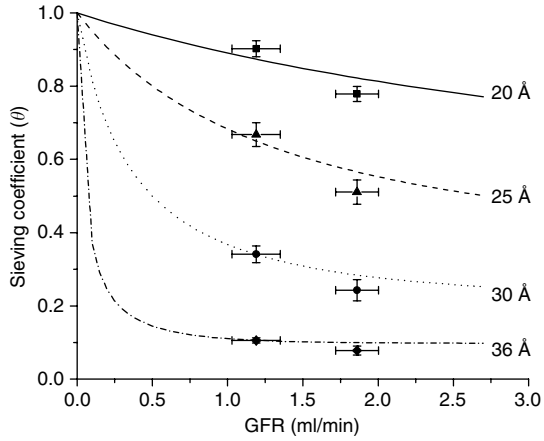

Figure 4 | Sieving coefficients as a function of GFR for four different Ficoll molecular radii compared with theoretical simulations using the two-pore theory setting r_s at 49.5 Å, r_L at 140 Å, $A_0/\Delta X$ at 390 000 cm, and α_L at 1×10^{-4}.

Table 1 | (a) Two-pore model analysis[a] and (b) log-normal distributed+shunt analysis of average θ vs a_e curves[b]

GFR (ml/min)	Small pore radius (r_s) (Å)	Large pore radius (r_L) (Å)	$A_0/\Delta X$ (cm)	J_{V_L}/GFR	$>\alpha_L$	Glomerular oncotic pressure ($\Delta\pi$) (mmHg)
(a) Two-pore model analysis						
1.16 ± 0.17	50.3 ± 0.38	136 ± 8.6	$3.73 \pm 0.85 \times 10^5$	$2.67 \pm 0.45 \times 10^{-4}$	$6.04 \pm 1.5 \times 10^{-5}$	28.0 ± 1.1
2.03 ± 0.17	48.9 ± 0.77	140 ± 11	$3.96 \pm 0.73 \times 10^5$	$2.51 \pm 0.45 \times 10^{-4}$	$7.45 \pm 1.5 \times 10^{-5}$	26.7 ± 0.9
GFR (ml/min)	Mean pore radius (u_l) (Å)	Distribution parameter (s_l)	$A_0/\Delta X$ (cm)	Jv_L/GFR	α_L	Glomerular oncotic pressure ($\Delta\pi$) (mmHg)
(b) Log-normal distributed+shunt analysis of average θ vs a_e curves						
1.16 ± 0.17	38.8 ± 0.79	1.19 ± 0.02	$1.04 \pm 0.12 \times 10^6$	$7.20 \pm 2.6 \times 10^{-5}$	$1.14 \pm 0.41 \times 10^{-5}$	28.0 ± 1.1
2.03 ± 0.17	38.8 ± 0.70	1.18 ± 0.01	$1.21 \pm 0.22 \times 10^6$	$6.98 \pm 1.5 \times 10^{-5}$	$1.83 \pm 0.21 \times 10^{-5}$	26.7 ± 0.9

[a]Analysis of Ficoll sieving data at the two GFR levels investigated using the two-pore model analysis of individual sieving curves. The oncotic pressures for the two GFRs are calculated as described in Lund *et al.*,[5] assuming that the (afferent arteriole) plasma oncotic pressure is 22 mmHg. α_L is calculated for *LpS*=0.22 (ml/min/mmHg), compatible with $A_0/\Delta X$ 1×10^6 cm. For J_{V_L}/GFR and α_L, n=7+3. For all other parameters, n=7.

[b]Parameters for the log-normal distributed model+shunt analysis. The calculations are based on Rippe and Haraldsson,[11] Deen *et al.*[20] and McNamee and Wolf[32] and are described in detail in Appendix A1.

DISCUSSION

This *in vivo* study demonstrates that the fractional clearances (θ) of Ficoll fractions in the radius range of 13–43 Å are reduced when GFR is raised from initially low values to higher (normal range) levels in hydropenic rats. The data agree with previous *in vivo* studies of θ vs GFR using either proteins or dextran as probes for testing the glomerular size selectivity.[5,8] Theoretically, if the main sieving barrier in the glomerular capillary wall were close to the plasma side, the effect of an increased GFR would be to reduce the diffusional component of transport, so that, eventually, at high GFRs, θ will fall to approach $(1-\sigma)$.[11,12] However, if the major sieving barrier were located at the PSD, then the reduction in θ will be counteracted by concentration polarization effects. The two opposing effects would largely cancel at low GFR levels, leaving θ unchanged when GFR is raised. However, at high GFRs, concentration polarization would dominate, tending to cause a rise in θ for macromolecules at high levels of GFR.[1,7] This was, however, not seen in the present study. The present data, demonstrating a fall in θ with GFR, are rather consistent with the glomerular barrier producing a size-separation effect 'early' in the filter.

The measured reduction in θ for Ficoll (13–43 Å in radius) was slightly larger than predicted by the two-pore theory (Figure 4). A major reason is that fitting measured Ficoll θ data to the two-pore theory underestimates the diffusive component ($A_0/\Delta X$) of transport. The low $A_0/\Delta X$ obtained for Ficoll ($\sim 400\,000$ cm) is a major factor contributing to the discrepancy between the predicted and experimental values. If the value for $A_0/\Delta X$ obtained using the log-normal distributed pore theory ($\sim 1.2 \times 10^6$ cm) or $A_0/\Delta X$ obtained using protein probes ($\sim 1.8 \times 10^6$ cm) was used instead, predictions became more accurate. While the diffusion component was sufficiently high for θ of Ficoll fractions in the range of 13–43 Å, to be markedly reduced with GFR elevations, the diffusional component is negligible for molecules approaching the small pore radius. Any increases in GFR will thus leave θ unaffected for such Ficoll fractions. Our data thus clearly demonstrate that there was no reduction in θ for molecules of radius between 45 and 60 Å (Figure 2b).

For molecules larger than 60 Å in radius, which, according to the two-pore model, are considered to pass through large pores only, convection would be the dominating transport mode. Here, increasing GFR will theoretically reduce the relative fluid flow occurring through large pores (J_{v_L}/GFR) and reduce θ, so that it, eventually, would approach $\alpha_L(1-\sigma_L)$.[16] In our study, we found a tendency toward a reduction in θ for very large Ficoll fractions (>70 Å in radius). However, because only very small amounts of high molecular radius material ($\theta < 10^{-4}$) passed through the assumed large pores, the data variability was very large for these molecules (cf. Figure 2b).

Applying the log-normal distributed pore model to the θ data, both r_s and $A_0/\Delta X$ were found to be similar to those measured for neutral protein probes. However, when the non-distributed two-pore model was employed, the small pore radius was considerably larger (49–50 Å) and $A_0/\Delta X$ was lower than measured using protein probes ($r_s = 37.5$ Å and $A_0/\Delta X = 1.8 \times 10^6$).[15] With dextran, the glomerular small pore radius has been determined to be even larger.[14,15] Dextran is an elongated, flexible, random-coil molecule that can pass through pores that are even smaller than the SE radius of the molecule itself.[13] Ficoll is a highly branched polysaccharide with a rather extensive internal crosslinking, making it much more spherical than most other polysaccharides. In spite of this, it still appears hyperpermeable *in vivo* as compared to globular proteins.[15,17,18]

During the past few decades, the transport of macromolecules across microvascular walls in a number of various tissues has usually been described using a two-pore model of membrane permeability.[11,12,19] According to this model, a large number of 'small pores' (of radius 40–50 Å) severely restrict the passage of macromolecules, while a very low number of 'large' pores (radius 160–300 Å) are only slightly protein restrictive. In 1985, the two-pore model was introduced in the context of glomerular transport,[20] although large pores were conceived as 'shunts'. In the present study, the two-pore model appeared to be inaccurate in describing Ficoll sieving data in the a_e interval 50–65 Å, while the log-normal distributed (plus shunt) model was not. Despite this fact, we do not believe that the glomerular barrier actually has a wide distribution of pores with a small number of shunts. Such a wide pore distribution, even considering the presence of negative pore charge, would not be consistent with the high selectivity to globular proteins normally characterizing the glomerular barrier.[5,10,21] Furthermore, shunts in the classical sense are unlikely to be present in the normal glomerulus. In rats, whose proximal tubular protein reabsorption was inhibited with lysine, it was demonstrated that the clearances of 'large' proteins were compatible with the presence of large pores of radius 110–120 Å.[16] Thus, θ declined in the order albumin > immunoglobulin (Ig)G > α_2-macroglobulin. IgM was not found in rat primary urine at all. Moreover, in the cooled isolated perfused kidney (cIPK), there is ample evidence for the presence of two populations of pores in the glomerular filter,[22] and application of the two-pore model makes it possible to compare the present results with those obtained in the cIPK.

Instead of the concept of a wide pore distribution in the glomerular filter, one has to consider the fact that carbohydrates, such as Ficoll and dextran, exhibit an 'extended' molecular conformation, partly correlated to their larger SE radius (compared to that for globular proteins) for any given molecular mass.[15] Such an extended configuration, conceivably, renders most carbohydrates more flexible (compressible) than any globular protein. It is likely that an increased flexibility makes carbohydrates behave differently compared to rigid proteins in the permeable pathways (pores).[13,15,17,18,23] *In vitro* experiments using Ficoll show that the molecules were indeed hyperpermeable when the Ficoll radii exceeded 40–50% of the pore radius in

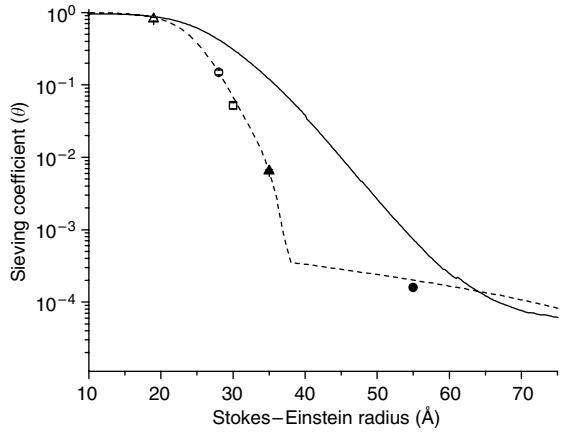

Figure 5 | Sieving coefficients for Ficoll (—) covering the whole spectrum of molecular radii from 10 to 75 Å are compared with sieving coefficients for some proteins, namely myoglobin ($a_e = 19.4$ Å; △), κ-dimer ($a_e = 28.4$ Å; ○), horseradish peroxidase ($a_e = 30.5$ Å; □), neutralized albumin ($a_e = 35$ Å; ▲), and IgG ($a_e = 54$ Å; ●). The protein data used for this comparison were assessed in earlier experiments from our laboratory.[5,16] Data for α_2-macroglobulin and IgM[5,16] are not shown. The best-fitting two-pore model curve was calculated to fit the protein data and plotted vs SE radius (---- curve) using the following parameters: $r_s = 37.5$ Å, $r_L = 125$ Å, $\alpha_L = 1 \times 10^{-4}$, and $A_0/\Delta X = 1.8 \times 10^{-6}$ cm.[5,16]

track-etched membranes.[13] Comparing our Ficoll sieving data with protein sieving data obtained previously in our laboratory in the same experimental setting,[5,16] it seems that small Ficoll molecules are not hyperpermeable across the small pores when $a_e/r_P < 0.5$ (Figure 5). However, with increasing SE radius (25–55 Å), there seems to be a progressive hyperpermeability of Ficoll, being maximal in the radius range of 40–60 Å. For Ficoll molecules larger than 60 Å, but smaller than 80 Å, there seems, however, again to be a good correspondence of Ficoll θ with protein θ. This is to be expected if large pores (of radius ~140–160 Å) or shunts exist, because in such large pores (or shunts) the a_e/r_p ratio would be <0.5 for 60–80 Å radius molecules, and hence, Ficoll would *not* be hyperpermeable under these conditions.

In contrast to our study, Ohlsson *et al.*[24] recently found in the cIPK that θ for Ficoll molecules of radius >45 Å increased, with increasing GFR, which was also true for albumin. Also, $A_0/\Delta X$ and α_L increased with increases in GFR, which was not observed in the present study. The reason for this discrepancy is not clear. However, in the cIPK, only ~10% of the nephrons are actually perfused, whereas the filtration fraction is only 0.05.[25] Furthermore, Jeansson *et al.*[26] showed that the number of large pores was markedly increased in the cIPK compared to the situation *in vivo*. Also, in the cIPK, θ for albumin progressively increased with perfusion time (and GFR elevations),[6,24] which adds to the difficulty in interpreting *in vitro* data of θ vs GFR. Conceivably, by increasing the perfusion pressure to raise GFR, this may recruit additional, potentially ischemic, nephrons with an increased glomerular permeability (increased α_L), thus explaining the increased θ (α_L) and $A_0/\Delta X$ as a function of increases in GFR. Again, it should be noted, however, that there is no significant difference among the Ficoll sieving curves in the a_e range up to 45 Å in the present study and those in the cIPK.[26,27] In fact, our results are in agreement with a multitude of recent Ficoll sieving data in man, rat, and mouse, from different laboratories, using different size separation systems and calibration methods for the Ficoll measurements.[15,27–31]

In conclusion, the sieving characteristics of the rat glomerular barrier to Ficoll were in the present study found to be consistent with previous *in vivo* measurements in man, mouse, and rat.[28–31] Furthermore, θ values for Ficoll fractions of radius 13–43 Å were reduced when GFR was increased. This reduction in θ for Ficoll indicates the presence of a high diffusive component of glomerular Ficoll filtration in rats *in vivo*. It seems to contradict the notion of a significant concentration polarization effect in the glomerular filter *vis-à-vis* Ficoll molecules <50 Å in radius. Furthermore, the glomerular small pore radius assessed from the present and previous Ficoll sieving data applying the two-pore theory, but not using the log-normal distributed pore model, was found to be considerably larger than that previously determined using neutral proteins as test molecules.

MATERIALS AND METHODS

Surgery

Experiments were performed in 10 male Wistar rats (Møllegaard, Lille Stensved, Denmark) weighing 304 ± 18 g (± s.e.). The rats were anesthetized intraperitoneally with 60 mg/kg sodium pentobarbital and were kept at 37°C. The left carotic artery, left jugular vein, and the tail artery were cannulated (PE-50) for infusion, blood sampling, and arterial pressure recordings on a polygraph (Model 7B, Grass Instruments, Quincy, MA, USA), respectively. After laparotomy, catheters (PE-10 coupled to a PE-50) were placed in the left and the right ureter used for urine collection. The Animal Ethics Committee at Lund University approved the studies.

Experimental protocol

Ficoll 70 (Pharmacia, Uppsala, Sweden) and Ficoll 400 (Sigma, St Louis, MO, USA) were labeled with fluorescein isothiocyanate (FITC) according to Olsson *et al.*[6] A mixture containing FITC-Ficoll 400 (1 mg), FITC-Ficoll 70 (42 μg), FITC-labeled inulin (500 ng) (TdB Consultancy, Uppsala, Sweden), and ^{51}Cr-ethylenediaminetetraacetic acid (EDTA) (0.09 MBq in 0.2 ml, Amersham, Biosciences, UK) was given as a priming bolus dose followed by a constant infusion of FITC-Ficoll 400 (3 mg/min), FITC-Ficoll 70 (94.5 μg/min), FITC-inulin (1.5 μg/min), and ^{51}Cr-EDTA (0.005 MBq/min). After a 20 min equilibration period, the first experiment with low (prevailing) GFR in the normal hydropenic rat was started. Urine was collected over a 5 min period and blood samples were collected at 0, 2.5, and 5 min. The radioactivity of ^{51}Cr-EDTA was measured using a gamma counter (Wizard 1480, LKB-Wallac, Turku, Finland). The GFR was raised by first volume loading the animals via an intravenous (i.v.) infusion of 4 ml horse serum (SVA, Uppsala, Sweden) over 1 min. Then, after 5 min, glucagon (Novo Nordisk, Denmark) (3 μg/min, i.v.) was added to the infusion to induce further increases in renal blood flow. At 5 min after the start of glucagon infusion, one additional milliliter of horse serum was

infused. In the first seven rats, we used the concentrations of Ficoll and inulin as described above. In three additional rats, we raised the concentration of FITC-Ficoll 400 10-fold in comparison to FITC-Ficoll 70 in an attempt to achieve more reliable θ data for the largest Ficoll fractions. A simple van't Hoff calculation based on the Ficoll average molecular weight showed that the contribution of Ficoll to the total plasma oncotic pressure was negligible at both 'low' (0.02%) and 'high' (0.35%) concentrations.

High-pressure size-exclusion chromatography

High-pressure chromatography was performed with devices from Waters (Milford, MA, USA). The system consists of pumps (Waters 1525), an absorbance detector (Waters 2487) and a fluorescence detector (Waters 2475). Size exclusion was achieved using an Ultrahydrogel-500 column (7.8 × 300 mm, Waters), and using a 0.05 M phosphate buffer with 0.15 M NaCl (pH 7.4) as mobile phase. The system was controlled using Breeze software 3.2 (Waters). As shown in Figure 6a, the column was calibrated with narrow Ficoll standards (73, 59, 46, 38, and 30 Å), which were kindly provided by Dr Torvald Andersson (Pharmacia, Sweden) and labeled as described above.

Calculations

θ for Ficoll. Values of θ were calculated by dividing primary urine Ficoll concentrations vs a_e with average Ficoll plasma concentrations (C_{p_F}). The primary urine concentration of Ficoll was obtained by dividing the (final) urine Ficoll concentration (C_{u_F}) by the final urine to plasma inulin concentration ratio ($C_{u_{in}}/C_{p_{in}}$).

$$\theta = \frac{C_{u_F} C_{p_{in}}}{C_{p_F} C_{u_{in}}} \quad (1)$$

GFR measurements. The steady-state clearance of inulin and ^{51}Cr-EDTA from plasma to urine was used to assess GFR and was calculated from

$$GFR = \frac{C_u V_u}{C_{pw}} \quad (2)$$

where C_u represents the urinary concentration of ^{51}Cr-EDTA or inulin, V_u represents the urine flow (ml/min) and C_{pw} is the plasma water concentration of ^{51}Cr-EDTA or plasma concentration of inulin.

Pore models. The pore models used in the present study are the two-pore model, which has been described previously,[5,11,16] and the log-normal distributed pore model (with a shunt), which is described in Appendix A1.

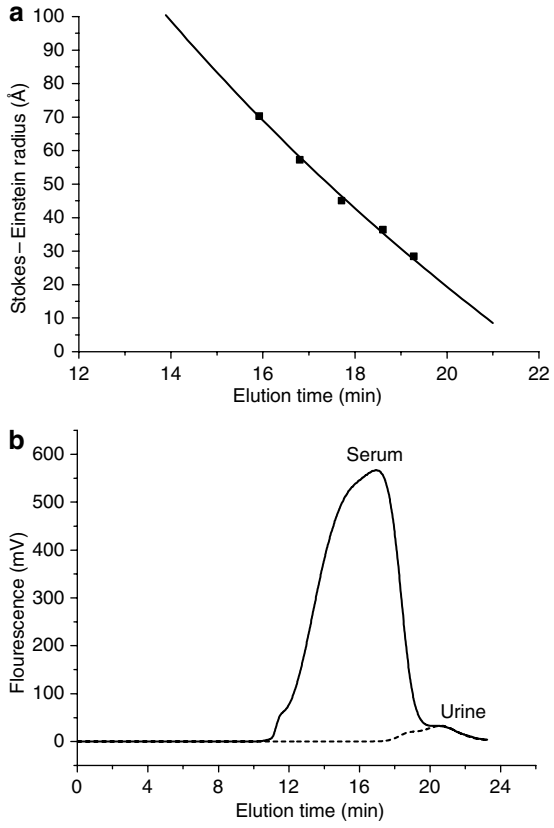

Figure 6 | (a) The Ultrahydrogel-500 column was calibrated using narrow Ficoll standards, labeled with FITC, and detected using a fluorescence detector. A calibration curve was obtained using the relationship $y = -222 \ln(x) + 685$. (**b**) Representative distribution curves from serum and primary urine (urine was recalculated to obtain Bowmans space concentration) after separation on size-exclusion chromatography.

Statistics

Values are given as means ± s.e. Experimental θ vs a_e curves were analyzed using either the two-pore model or the log-normal distributed pore model with a shunt. The best fit was obtained using non-linear least-squares regression analysis using scaling multipliers as described previously.[5] For a majority of curves, Ficoll data for a_e 59–69 (Å) were excluded when applying the two-pore analysis, but not using the log-normal distributed pore analysis, owing to relatively poor fit of θ data to the two-pore theory in this radius interval ('knee' region of the θ vs a_e curve).

ACKNOWLEDGMENTS

We are grateful to Kerstin Wihlborg for skillfully typing the manuscript. This work was supported by Swedish Medical Research Council Grant 08285, the Lundberg Medical Foundation, European Union Contract FMRX-C98-2019 and Lars Hierta Memorial Foundation.

REFERENCES

1. Deen WM, Lazzara MJ, Myers BD. Structural determinants of glomerular permeability. *Am J Physiol Renal Physiol* 2001; **281**: F579–F596.
2. Tryggvason K. Unraveling the mechanisms of glomerular ultrafiltration: nephrin, a key component of the slit diaphragm. *J Am Soc Nephrol* 1999; **10**: 2440–2445.
3. Ohlson M, Sörensson J, Haraldsson B. A gel-membrane model of glomerular charge and size selectivity in series. *Am J Physiol Renal Physiol* 2001; **280**: F396–F405.
4. Rodewald R, Karnovsky MJ. Porous substructure of the glomerular slit diaphragm in the rat and mouse. *J Cell Biol* 1974; **60**: 423–433.
5. Lund U, Rippe A, Venturoli D *et al.* Glomerular filtration rate dependence of sieving of albumin and some neutral proteins in rat kidneys. *Am J Physiol Renal Physiol* 2003; **284**: F1226–F1234.
6. Ohlson M, Sörensson J, Haraldsson B. Glomerular size and charge selectivity in the rat as revealed by FITC-Ficoll and albumin. *Am J Physiol Renal Physiol* 2000; **279**: F84–F91.
7. Edwards A, Daniels BS, Deen WM. Ultrastructural model for size selectivity in glomerular filtration. *Am J Physiol* 1999; **276**: F892–F902.
8. Chang RL, Ueki IR, Troy JL *et al.* Permselectivity of the glomerular capillary wall to macromolecules. *Biophys J* 1975; **15**: 887–906.
9. Patlak CS, Goldstein DA, Hoffman JF. The flow of solute and solvent across a two-membrane system. *J Theor Biol* 1963; **5**: 426–442.
10. Renkin EM, Gilmore JP. Glomerular filtration. In: Orloff J, Berliner RW (eds). *Handbook of Physiology. Renal Physiology*. American Physiological Society: Washington, DC, 1973, pp 185–248.
11. Rippe B, Haraldsson B. Transport of macromolecules across microvascular walls. The two-pore theory. *Physiol Rev* 1994; **74**: 163–219.

12. Taylor AE, Granger DN. Exchange of macromolecules across the microcirculation. In: Renkin EM, Michel CC (eds), *Handbook of Physiology. The Cardiovascular System. Microcirculation*, Section 2, vol. IV, Chapter 11. American Physiological Society: Bethesda, MD, 1984: 467pp.
13. Bohrer MP, Patterson GD, Carroll PJ. Hindered diffusion of dextran and Ficoll in microporous membranes. *Macromolecules* 1984; **17**: 1170–1173.
14. Bohrer MP, Deen WM, Robertson CR, *et al.* Influence of molecular configuration on the passage of macromolecules across the glomerular capillary wall. *J Gen Physiol* 1979; **74**: 583–593.
15. Venturoli D, Rippe B. Ficoll and dextran vs. globular proteins as probes for testing glomerular permselectivity: effects of molecular size, shape, charge, and deformability. *Am J Physiol Renal Physiol* 2005; **288**: F605–F613.
16. Tencer J, Frick IM, Öqvist BW *et al.* Size-selectivity of the glomerular barrier to high molecular weight proteins: upper size limitations of shunt pathways. *Kidney Int* 1998; **53**: 709–715.
17. Lavrenko PN, Mikriukova OI, Okatova OV. On the separation ability of various Ficoll gradient solutions in zonal centrifugation. *Anal Biochem* 1987; **166**: 287–297.
18. Teraoka I. Polymer solutions in confining geometries. *Prog Polym Sci* 1996; **21**: 89–149.
19. Renkin EM. Capillary transport of macromolecules: pores and other endothelial pathways. *J Appl Physiol* 1985; **58**: 315–325.
20. Deen WM, Bridges CR, Brenner BM *et al.* Heteroporous model of glomerular size selectivity: application to normal and nephrotic humans. *Am J Physiol* 1985; **249**: F374–F389.
21. Norden AG, Lapsley M, Lee PJ *et al.* Glomerular protein sieving and implications for renal failure in Fanconi syndrome. *Kidney Int* 2001; **60**: 1885–1892.
22. Haraldsson B, Sörensson J. Why do we not all have proteinuria? An update of our current understanding of the glomerular barrier. *News Physiol Sci* 2004; **19**: 7–10.
23. Wenner JR, Bloomfield VA. Crowding effects on *Eco*RV kinetics and binding. *Biophys J* 1999; **77**: 3234–3241.
24. Ohlson M, Sörensson J, Lindström K *et al.* Effects of filtration rate on the glomerular barrier and clearance of four differently shaped molecules. *Am J Physiol Renal Physiol* 2001; **281**: F103–F113.
25. Lindström KE, Rönnstedt L, Jaremko G *et al.* Physiological and morphological effects of perfusing isolated rat kidneys with hyperosmolal mannitol solutions. *Acta Physiol Scand* 1999; **166**: 231–238.
26. Jeansson M, Haraldsson B. Glomerular size and charge selectivity in the mouse after exposure to glucosaminoglycan-degrading enzymes. *J Am Soc Nephrol* 2003; **14**: 1756–1765.
27. Hjalmarsson C, Ohlson M, Haraldsson B. Puromycin aminonucleoside damages the glomerular size barrier with minimal effects on charge density. *Am J Physiol Renal Physiol* 2001; **281**: F503–F512.
28. Andersen S, Blouch K, Bialek J *et al.* Glomerular permselectivity in early stages of overt diabetic nephropathy. *Kidney Int* 2000; **58**: 2129–2137.
29. Oliver III JD, Simons JL, Troy JL *et al.* Proteinuria and impaired glomerular permselectivity in uninephrectomized fawn-hooded rats. *Am J Physiol* 1994; **267**: F917–F925.
30. Guimaraes MA, Nikolovski J, Pratt LM *et al.* Anomalous fractional clearance of negatively charged Ficoll relative to uncharged Ficoll. *Am J Physiol Renal Physiol* 2003; **285**: F1118–F1124.
31. Blouch K, Deen WM, Fauvel JP *et al.* Molecular configuration and glomerular size selectivity in healthy and nephrotic humans. *Am J Physiol* 1997; **273**: F430–F437.
32. McNamee JE, Wolf MB. Prediction of permeability-surface area product data by continuous-distribution pore models. *Microcirculation* 1998; **5**: 275–280.
33. Mason EA, Wendt RP, Bresler EH. Similarity relations (dimensional analysis) for membrane transport. *J Membr Sci* 1980; **6**: 283–298.

Appendix A1
Distributed model

The experimental data were described by a two-pore model according to Lund *et al.*,[5] Rippe and Haraldsson[11] and Tencer *et al.*[16] and a distributed pore model based on Rippe and Haraldsson,[11] Deen *et al.*,[20] and McNamee and Wolf.[32] For the distributed model with a shunt, the measured sieving profiles were considered as originating from an unselective shunt in parallel to a log-normal distribution of membrane pores, with parameters u (mean pore radius) and s (distribution width), according to

$$g(r) = \frac{1}{\sqrt{2\pi}r\ln(s)} \exp\left[-\frac{1}{2}\left(\frac{\ln(r)-\ln(u)}{\ln(s)}\right)^2\right] \quad (A1)$$

By assuming a Poiseullian regime for the fluid flow through the pores, the distributed reflection coefficient can be calculated as

$$\sigma_D(a_e) = \frac{\int_0^\infty r^4 g(r)\sigma_h(a_e, r)dr}{\int_0^\infty r^4 g(r)dr} \quad (A2)$$

where a_e is the SE radius and $\sigma_h(a_e, r)$ is the homoporous reflection coefficient given by equation (3) in Tencer *et al.*[16,33] The corresponding permeability–surface area product (PS) is

$$PS_D(a_e) = \frac{\int_0^\infty r^2 g(r)\frac{A}{A_0}(a_e, r)\frac{A_0}{\Delta x}D_\infty(a_e)dr}{\int_0^\infty r^2 g(r)dr} \quad (A3)$$

where $A_0/\Delta x$ is the area over diffusion distance parameter, $D_\infty(a_e)$ is the (water) free diffusion coefficient of a molecule of size a_e, calculated at 37°C[11] as

$$D_\infty(a_e) = \frac{3.243\times10^{-5}}{a_e} \quad (A4)$$

and A/A_0 is the degree of restricted diffusion according to equation (8) in Tencer *et al.*[16,33] Theoretically, all the integrals in this model should be calculated over the interval $(0, \infty)$. Numerically, however, the integrals were estimated between the radius of a water molecule, a_w (2 Å),[33] and r_{MAX}, where r_{MAX} represents the minimum r value after which the integral numerical value stays constant while r increases.[20]

The Peclet number for the distributed portion has been calculated as

$$Pe(a_e, GFR) = \frac{(1-f_L)GFR(1-\sigma_D(a_e, r))}{PS_D(a_e)} \quad (A5)$$

where f_L represents the fraction of fluid flow crossing the membrane through the shunt.

The θ for the whole membrane can then be calculated as

$$\theta_D(a_e, GFR) = \frac{1-\sigma_D(a_e)}{1-\sigma_D(a_e)\exp(-Pe(a_e, GFR))} + f_L \quad (A6)$$

Best fit. The theoretical θ values were adapted to the experimental data by a modified least-squares method, defining the objective function as follows:

$$\chi = \sum_{a_e}\left(1-\frac{\theta_{th}}{\theta_{exp}}\right)^2 \quad (A7)$$

where θ_{exp} is the measured sieving curve, $\theta_{th} = \theta_D(a_e, GFR)$, and the sum is carried over all of the measured a_e.

The values of the parameters u, s, $A_0/\Delta x$, and f_L minimizing the objective function were considered corresponding to the 'best fit'.